Design of a high-voltage electrostatic ultrasonic atomization nozzle and its droplet adhesion effects on aeroponically cultivated plant roots

Jianmin Gao*, Yinan Guo, Mazhar Hussain Tunio, Xiangchao Chen, Zhijian Chen
(*School of Agricultural Engineering, Jiangsu University, Zhenjiang 212013, Jiangsu, China*)

Abstract: In the process of aeroponics cultivation, the atomizer is one of the most important influencing factors on the cultivation process. This study presented the design of an ultrasonic atomization nozzle using contact charging and a root droplet adhesion test rig. The purpose of this study was to reveal the relationship between the main operating parameters of the high-voltage electrostatic ultrasonic atomization nozzle and the atomization effect using droplet adhesion measurements. In this study, the ultrasonic effect of nozzle was achieved by using Laval tube, and the design of the key parameters for the high-voltage electrostatic ultrasonic atomization nozzle were inlet pressure, electrostatic voltage root core electrode material and spray distance; the droplet size variation and root adhesion patterns were obtained through experiments. The best operating parameters were analyzed by using the orthogonal test method, and the droplet deposition distribution of the root system at different scales was investigated in the atomization chamber. The test results revealed that when the root core electrode material was coppe and the nozzle working parameters were at 0.4 MPa of inlet pressure, at 1.75 m the spray distance, at 12 kV of the electrostatic voltage, the root system has the highest droplet adhesion.

Keywords: ultrasonic nozzle, high pressure electrostatic system, droplet size measurement, root adhesion test, droplet deposition effect
DOI: 10.25165/j.ijabe.20231602.7222

Citation: Gao J M, Guo Y N, Tunio M H, Chen X C, Chen Z J. Design of a high-voltage electrostatic ultrasonic atomization nozzle and its droplet adhesion effects on aeroponically cultivated plant roots. Int J Agric & Biol Eng, 2023; 16(2): 30–37.

1 Introduction

Aeroponics technology is a new method of soilless cultivation method. Crops grow by absorbing nutrient droplets that stick to root systems, thereby meeting the need of plant cultivation for water and fertilization conservation[1,2]. In an aeroponics system the nozzles play a major role in plant growth[3]. The lack of soil resistance in the cultivation process reduces the efficiency of the root system to absorb the nutrients[4,5], while studies have shown that electrostatic spraying can make the droplets better adhere to the root system due to its characteristics compared with ordinary spraying[6]. Therefore, it is necessary to investigate the influence of different operating parameters on droplet characteristics during the atomization process of the high-voltage electrostatic ultrasonic spray nozzle.

Al-mamury et al.[7] studied the coverage of fog droplets ejected from induction charging nozzles deposited on target surface under the action of electric field force, and used COMSL software to analyze the action of electrostatic field force on different targets (conical, flat, cylindrical, elliptic and spherical). Bren et al.[8] proposed a new method for estimating the droplet charge in numerical simulations of conduction and induction of electrospray. This method is based on balancing effective electric field at the sprayer nozzle with the global electric field induced by the charged droplets and is verified according to the experimental data in the paper, showing that the method can predict the droplet charge of conductive spray liquids with good accuracy over a wide range of spray parameters. Herrada et al.[9] and Wei et al.[10] proposed to use numerical simulations to accurately describe the flow patterns and jet characteristics of the entire liquid domain, and predicted the droplets diameter emitted from the tip of the cone jet. The fluid-based volume method simulates the feasibility of jet breakup and droplet formation. Laryea et al.[11] designed an electrostatic pressure cyclone nozzle for orchard spraying, based on the principle of electrostatic induction to make the droplets inductively charged. This phenomenon was shown experimentally that the nozzle has advantages of low pesticide input, high coverage, and low drift. Pascuzzi et al.[12] used the 150RB14 air-assisted electrostatic spray system of ESS to conduct a pilot study of spray deposition in trellised vineyards. The results showed that compared with non-electrostatic spraying, electrostatic spraying effectively increased the density and uniformity of droplet deposition within the canopy at the same height, but increased and decreased the penetration of droplets. Patel et al.[13] designed an air-assisted electrostatic nozzle and conducted an experimental study on the influence of air pressure, electrostatic voltage, spray distance, media conductivity and other factors on the droplet charge-to-mass ratio and deposition mode. The results showed that the operating parameters had significant impacts on the droplet charge-to-mass ratio and deposition distribution pattern of the electrostatic nozzle. By optimizing the operating parameters, the spray performance and deposition effect of the electrostatic nozzle could be effectively improved. Later Patel et al.[14] developed an electrostatic nozzle for spraying on the cotton crops and verified its performance, and compared it with an imported electrostatic nozzle and a conical nozzle. Different spray performance parameters were determined by collecting the deposition of droplets by using water-sensitive paper

Received date: 2021-11-29 **Accepted date:** 2022-03-27
Biographies: Yinan Guo, Master candidate, research interest: fog tilling, Email: 1739680364@qq.com; **Mazhar Hussain Tunio**, PhD candidate, Lecturer, research interest: irrigation engineering, Email: mazharhussaintunio@sau.edu.pk; **Xiangchao Chen**, Master candidate, research interest: machine design, Email: 2541481918@qq.com; **Zhijian Chen**, PhD candidate, research interest: agriculture machine design, Email: 1178262202@qq.com.
***Corresponding author: Jianmin Gao**, Professor, research interest: soil and fog tilling. No 301, Xuefu Road, Zhenjiang 212013, Jiangsu, China; Tel: +86-13655282069, Email: gaojianminujs@163.com.

(WSP). The results showed that there was no significant difference in the performance of the two electrostatic nozzles, but they were more effective than the conical nozzle.

The literature indicates that electrostatic systems and spray characteristics have been studied to a certain extent. However, these studies on the corresponding macroscopic spray characteristics in the high-voltage electrostatic ultrasonic atomization spraying process are not enough. Furthermore, considering the significant differences in the physical properties of electrostatic and conventional sprays, the effect of droplet state on spray root adhesion formation under different conditions may be completely different from that of conventional sprays, so it is important to analyze the effect of electrostatic spraying of spray nozzles using root adhesion tests.

Therefore, the main purpose of this research article is to design the atomization nozzle using the supersonic tube principle and a high-voltage electrostatic system. The experimental study was conducted on the droplet adhesion effect, by comparing the droplet particle size, deposition quality and droplet deposition coverage under different parameters. It was also described the variation law of spray characteristics and atomization effect to make the atomizer operate more efficiently.

2 Materials and methods

2.1 Ultrasonic nozzle and high-speed airflow design

The authors have designed the atomization nozzles required for aeroponics, which are more effective in terms of droplet particle size and uniformity of particle size distribution[15]. However, the above-mentioned nozzle has complex structures, and high cost, which are not conducive to the popularization of aeroponics technology. Therefore, the authors designed a simple structure, reliable performance, low cost and insulation. The structural schematic diagram of the nozzle is shown in Figure 1.

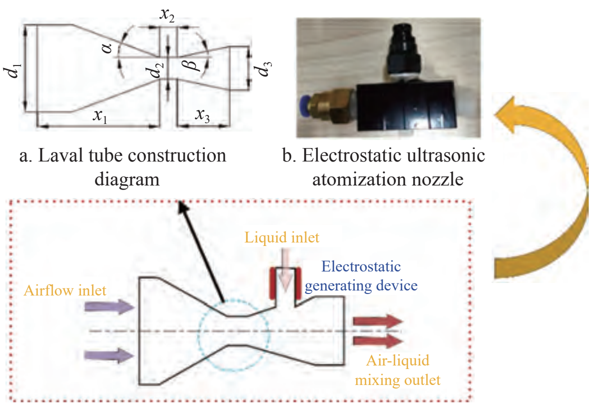

Figure 1 Schematic diagram of the nozzle construction scheme

2.1.1 Laval nozzle principle

The Laval nozzle is a typical energy conversion device. This kind of pipe whose profile shrinks first and then expands has been widely used in aerospace, supersonic wind tunnel, ultra-fine powder preparation, light industry, textile and other fields[16]. To realize the study of the relevant parameters of the supersonic nozzle, the fluid flow inside the tube is considered as isentropic flow. The changes in gravity, heat transfer and other factors are ignored, and only considering the change of cross-sectional is considered[17], which is derived from the continuity equation:

$$\rho v A = R \tag{1}$$

where, ρ is the gas density, kg/m^3; v is the gas velocity, m/s; A is the Laval tube cross-sectional area, m^2; R is a constant.

For one-dimensional in viscid isentropic flow, when the gas flows at a distance ds, the increase in velocity is dv and the increase in pressure is dp, then the gas flow process satisfies the momentum as Equation (2):

$$\iint_{A_2} v_2 \rho v_{2n} \mathrm{d}A - \iint_{A1} v_1 \rho v_{2n} \mathrm{d}A = \sum F \tag{2}$$

Also express the ratio of the gas velocity (v) to the speed of sound (c) at a given cross-section in the pipe according to the Mach number (M), the differential equation can be expressed as,

$$\frac{\mathrm{d}p}{p} = -\frac{\rho}{p} v \mathrm{d}v = -\gamma M^2 \frac{\mathrm{d}v}{v} \tag{3}$$

The logarithmic differential equation for the isentropic flow equation is

$$\frac{\mathrm{d}p}{p} = \gamma \frac{\mathrm{d}\rho}{\rho} \tag{4}$$

The logarithmic differential equation for the ideal gas equation of state $\rho v = nRT$ can be expressed as,

$$\frac{\mathrm{d}p}{p} = \frac{\mathrm{d}\rho}{\rho} + \frac{\mathrm{d}T}{T} \tag{5}$$

Combining Equations (2), (4) and (5) yields, then, Equation (6) could be got.

$$\frac{\mathrm{d}T}{T} = -(\gamma - 1) M^2 \frac{\mathrm{d}v}{v} \tag{6}$$

where, p is the gas pressure, Pa; M is the Mach number; T is the gas temperature, K; γ is the adiabatic index.

From the above theoretical analysis, to continuously expand the subsonic flow to supersonic flow, not only to meet the above conditions but also need to maintain a certain pressure difference between the two ends of the nozzle, that is, the Laval tube must achieve supersonic flow at the exit, the inlet pressure must be stronger than the nozzle exit section gas pressure.

2.1.2 Nozzle size experienced design

The structural design of the Laval tube consists of four main sections: stabilization section, contraction section, over section and expansion section[18,19]. The main design parameters are inlet diameter d_1, throat diameter d_2, outlet diameter d_3, contraction angle α, and expansion angle β.

The throat diameter d_2 of the Laval tube[20] was designed according to Equation (7).

$$\frac{\pi}{4} d_2^2 = Q_{m0} \frac{\sqrt{T_0}}{P_0} \left[\frac{k}{R} \left(\frac{2}{k+1} \right)^{\frac{k+1}{k-1}} \right]^{-\frac{1}{2}} \tag{7}$$

where, p_0 is the nozzle inlet pressure, Pa; k is the adiabatic index; R is the gas constant; Q_{m0} is the nozzle inlet air mass flow, kg/s; T_0 is the nozzle inlet temperature, K.

Since most of aeroponics is carried out under constant temperature conditions, the ambient temperature of aeroponics is taken to be 25°C. According to the air and pressure relationship table can be obtained, when the pressure was 0.4 MPa, the air density was 4.6764 kg/m^3, at that time the air compressor stable working mass flow rate for the air density was 3.5073×10^{-3} kg/s, brought into the formula can be obtained: d_2 = 2.5 mm.

The airflow velocity at the inlet of the Laval tube is not large, and for supersonic wind tunnels, a smooth continuous shrinkage surfaces (Vito Shinseki formula) are used to reduce flow losses[21] for design.

$$R = \frac{R^2}{\sqrt{1-\left[1-\left(\frac{R_2}{R_1}\right)^2\right]^2 \frac{\left(1-x^2\right)^2}{\left(1+\frac{x^2}{3}\right)^3}}} L \tag{8}$$

where, R is the radius of the nozzle constriction section, mm; R_1 is the inlet radius, mm; R_2 is the throat radius, mm; x is the relative coordinate.

Considering, the high processing difficulty of this design method, to facilitate processing, the contraction section is a straight line. The experiments have proved that the uniformity of flow field can be maintained better when the inclination angle is selected 20°-45°. In this research， based paper 30° is chosen as the contraction angle α. Meanwhile, to ensure the uniformity of the airflow into the throat, the Laval inlet diameter is 3-5 times the throat diameter. Hence, in this study the inlet diameter was chosen $d_1 = 4d_2$; however, the inlet diameter d_1 is 10 mm. The length of the contraction section can be obtained by calculation $x_1 = 14$ mm.

The design of the Laval expansion section line profile utilizes the conical nozzle design method[22], based on the outlet cross-sectional area equation.

$$d_3 = 0.66 d_2 \times (2.07)^{\lg B} \tag{9}$$

where, B is the inner and outer pressure ratio formula, with the value of 12.5, so the Laval tube outlet diameter of $d_3 = 3.665$ mm, for the convenience of processing to take $d_3 = 3.5$ mm.

The expansion section is linear, and the expansion angle is noted as β. The length of the expansion section x_3 is:

$$x_3 = \frac{d_3 - d_2}{2\tan(\beta/2)} \tag{10}$$

where, β is taken as 10°, giving $x_3 = 5.715$ mm, for ease of machining take $x_3 = 6$ mm.

The structure of the Laval tube designed according to the above formula is shown in Figure 1a and the final machined ultrasonic atomization nozzle is shown in Figure 1b.

2.2 High voltage electrostatic system design

There are two main fixing rings used to hold crops in mist culture, the lengths are 3 cm and 4 cm respectively, however, mist culture crops had more developed root system, the root of lettuce can reach up to 50 cm at maturity and had dense root growth. It is therefore when spraying, the roots tend to stick together, as shown in Figure 2, and it is often difficult to achieve droplet adhesion within the root system. Therefore, a root core electrode is designed. The electrodes are made up of spiral metal with a length of about 25 cm. It can be used with the fixing ring, as shown in Figure 3. Its main functions are:

Figure 2 Mist grown lettuce root system

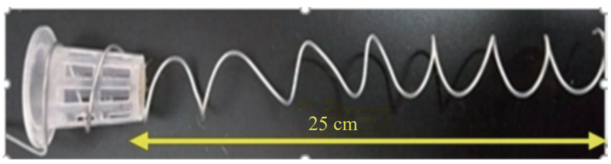

Figure 3 Root core electrode

1) During the crop maturity period, it can guide the growing root system to separate, to create space inside the root system to increase the adhesion area with the atomization droplets;

2) Aeroponics usually used to place the crop fixing plate is generally polyethylene foam plate, if the atomization droplets are negatively charged, and atomization crop roots in electrostatic induction will induce a positive charge, while the leaf part will gather more negative ions. If the atomization droplets contract the roots, the negative ions carried by the atomization droplets will neutralize the positive ions on the root system, due to air and polyethylene foam board for insulating material, the negative ions on the leaf cannot be neutralized with the positive ions generated by high-voltage electrostatic grounding. Theoretically the crop will be negatively charged, which is inconsistent with the facts. Therefore, to transfer the negative ions from the crop to the ground, the root core electrode is connected to the grounding wire.

Compared to other charging methods, contact charging has the best charging effect, the charging electrode material is used brass, and the charging position is selected at the nozzle entrance.

2.3 Numerical simulation of electrostatic droplets

The droplets produced during electrostatic spraying are small and uniform in size, in addition, the electrostatic droplets move towards the target under the force of the electric field, which can increase the amount of target deposition and deposition uniformity, and also have an effect on the amount of deposition on the back of plant leaves and inside the canopy[23], therefore an analysis of the droplet properties in an electrostatic field is required. The deformation and fragmentation of droplets is mainly affected by the electric field force, but also by the action of the surrounding flow field, this paper uses the coupled multi-physics analysis software COMSOL Multiphysics to numerically simulate the deformation and fragmentation process of droplets. As shown in Figure 4, a simulation model was created. The droplet is defined as a smooth ball, so the simulation model is symmetrical, and to reduce the simulation time, the simulation model is chosen to be two-dimensional. The upper and lower boundaries are the polar plates, the length of the plates is 50 mm, the spacing between the plates is 10 mm and the droplet is a circle with a diameter of 3 mm, the center of the circle is 5 mm from the left side entrance and 5 mm from the upper and lower plates.

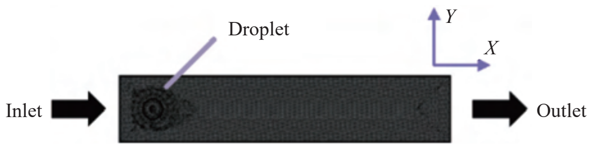

Figure 4 Grid distribution diagram

The two-phase parameters in the model are set as listed in Table 1. Simulations were carried out based on Laminar two-phase flow, with the phase field interfaces of the continuous and dispersed phases according to the Navier-Stokes equations

Table 1 Two-phase parameters

Materials	Density/ $kg \cdot m^{-3}$	Viscosity/ $mPa \cdot s$	Electrical conductivity/ $S \cdot m^{-1}$	Relative dielectric constant
Water	998	1	1.75	80
Air	1.29	1810	0	1.000 585

2.4 Root droplet adhesion testbed design

In this study, the performance of the high-voltage electrostatic ultrasonic atomization nozzle under different operating parameters was studied. As shown in Figure 5, the test ring consists of an aeroponics chamber, air compressor, high-voltage electrostatic spraying system, liquid storage tank, and a return pipe. The entire test bench is a wooden structure, which is mainly divided into two parts: the upper part is the aeroponics chamber, with the size of 150 cm×88 cm×88 cm, and it is covered with a fixed board of 2cm thick around and on the top. The front window is kept to mainly use for observation and operation. A water outlet is also installed to connect the return pipe to recycle the nutrient solution deposited on the wall. The fixing plate is equipped with test objects, each test object is connected by wires and finally grounded. The lower part is the supporting structure, which can accommodate an air compressor, diaphragm pump, high-voltage electrostatic module and water tank. The thermal anemometer (HT-9829) measures the airflow velocity at the nozzle outlet axis at 0.2 MPa, 0.3 MPa and 0.4 MPa respectively, and the airflow velocity is between 1.50-2.25 m away from the nozzle.

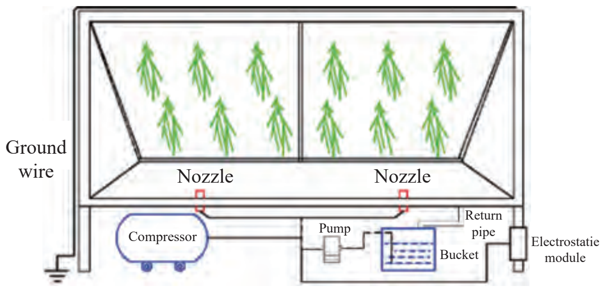

a. Schematic diagram of test bed

b. Different position views

Figure 5 Root droplet adhesion test bed

3 Experiments

3.1 Droplet size measurement test

The droplet size plays an important role in the deposition effect. In this study, a laser particle size analyzer was used to test the droplet size of the high-voltage electrostatic ultrasonic atomization nozzle, mainly for two factors of inlet pressure and electrostatic voltage. The temperature and relative humidity in the atomization chamber during the test were 10°C and 55% respectively. Before starting the test, the laser particle size analyzer was preheated for 30 min; the alignment was adjusted without adding the sample to be tested, and the relevant parameters were set after the adjustment was completed; the nozzle was fixed on the support, default values of pump parameters during the test (0.85 L/min, 0.4 MPa), and the nozzle was about 50 cm away from the laser particle size analyzer; While it should be in the same plane with the laser emitted by the laser particle size analyzer as much as possible; the inlet pressure P (0.2 MPa, 0.3 MPa, and 0.4 MPa) were adjusted. The electrostatic voltage U (0 kV, 6 kV, 8 kV, 10 kV, 12 kV) values for each spray case were measured three times, each time 5 s. To take the average of three samples, it was observed the grain size change pattern. The experimental setup at the test site is shown in Figure 6.

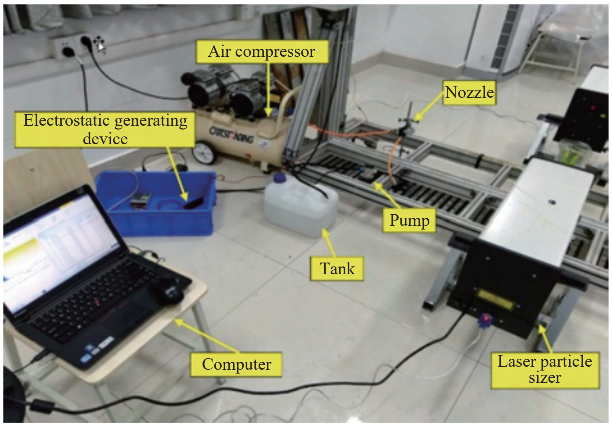

Figure 6 Droplet size measurement site

Taking the median diameter of the volume distribution D50 as the measurement index of the droplet diameter, the measured results are shown in Figure 7. It can be seen from the graph, when the inlet pressure P is 0.2 MPa, the average droplet size reaches 500 μm without applying electrostatic voltage, and when 12 kV electrostatic voltage was applied, the average droplet size showed below 300 μm. Compared with the former, the average droplet size was reduced by nearly half, because when an electrostatic voltage is applied, the high voltage electrostatic charge is applied to the droplet, and the electric field force exerted by the electrostatic field between the nozzle and the ground on the charged droplet causes the droplet to continue to break up. When the electrostatic voltage U was 0, the inlet pressure P was 0.3 MPa under the average particle size of the droplet than 0.2 MPa under the average particle size of the droplet reduced to about 80 μm. The reason is that the gas flow through the Laval tube accelerated into a high-speed airflow, the impact of high-speed airflow on the droplet increases the surface disturbance of the droplet, and the surface tension was not enough to maintain the droplet shape and thus deform and break. When the inlet pressure p was 0.4 MPa and the electrostatic voltage U was 12 kV, the minimum droplet particle size of 219.1 μm was observed.

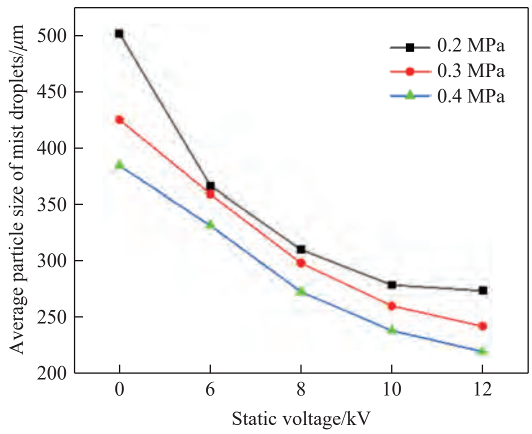

Figure 7 Droplet size measurement results

3.2 Root adhesion test and multi-factor orthogonal optimization

The test was conducted at a room temperature of 28°C-31°C and air humidity of 65%. The test subject was mature eelgrass with a steam height of about 38 cm when erect; the upper part of the plant stem was cut short and was kept at about 15 cm, the rest was covered with a sealing bag during the test. The bag was removed during weighing to reduce the errors caused during spraying and weighing. The root length of the plant was about 18 cm and the distance between the test plant and nozzle was about 2 m. The inlet pressure *P*, electrostatic voltage *U* and root core electrode material were selected as the three test factors. Among them, the inlet pressure *P* and root core electrode material were selected for three levels, and the electrostatic voltage *U* for six levels. Specific parameters are shown in Table 2.

Table 2 Test parameters

Test factors	Test level
Inlet pressure *P*/MPa	0.2, 0.3, 0.4
Electrostatic voltage *U*/kV	0, 6, 8, 10, 12, 14
Root-core electrode material	PVC, Al, Cu

Firstly, the influence of inlet pressure *P*, and electrostatic voltage *U* on the root droplet adhesion performance without the root core electrode was measured, and the experimental data are listed in Table 3. It can be seen from the table data, that when the electrostatic voltage was 0 kV and the inlet pressures were 0.2 MPa, 0.3 MPa and 0.4 MPa respectively, the corresponding root droplet adhesion amounts were 0.205 g, 1.164 g and 2.932 g, respectively. The increase in droplet adhesion was obvious, indicating that the increase in inlet pressure not only makes the droplet particle size finer, but also can transport the droplet to a farther target under the influence of airflow. The root droplet adhesions under the inlet pressure at 6 kV were 0.387 g, 1.683 g and 3.387 g, respectively. Compared with non-electrostatic spraying, the root droplet adhesion was significantly increased.

Table 3 Root atomization droplet adhesion

Inlet pressure *P*/MPa	Electrostatic voltage *U*/kV	Root adhesion increment Δm/g
0.2	0	0.205
	6	0.387
	8	0.490
	10	0.443
	12	0.610
	14	0.973
0.3	0	1.164
	6	1.683
	8	1.760
	10	2.137
	12	2.282
	14	2.500
0.4	0	2.932
	6	3.387
	8	3.910
	10	3.935
	12	4.183
	14	4.367

From the above results, it can be concluded that the inlet pressure *P* has a more obvious influence on the root adhesion volume, because the target was far away from the nozzle, and the gas pressure was too small resulting in the adhesion volume being small, and was difficult to distinguish. Therefore, the inlet pressure was fixed at 0.3 MPa, measuring the influence of different electrostatic voltage *U* and root core electrode material on the root adhesion performance, the specific test data are listed in Table 4. The test results show that the minimum values of root droplet adhesion were 1.164 g, 1.545 g, and 1.577 g when the root core electrode material was PVC, aluminum and copper respectively. However, the maximum values of root droplet adhesion were 2.5 g, 3.313 g and 3.545 g, respectively.

Table 4 Root atomization droplet adhesion

Root core electrode material	Electrostatic voltage *U*/kV	Root adhesion increment Δm/g
PVC	0	1.164
	6	1.683
	8	1.76
	10	2.137
	12	2.282
	14	2.5
Al	0	1.545
	6	1.987
	8	2.543
	10	2.806
	12	3.167
	14	3.313
Cu	0	1.577
	6	2.274
	8	2.703
	10	3.115
	12	3.3
	14	3.545

Since there are many factors affecting root droplet adhesion, including spray distance *L*, and inlet pressure *P*. The effects of each two factors are only discussed above. If the above factors can be more optimally combined, the quality of the mist cultivated crop will be improved. Therefore, the multi-factor orthogonal test method was used to test the root droplet adhesion.

The inlet pressure *P*, the electrostatic voltage *U*, root core electrode material and spray distance L were used as the four test factors, and three levels were taken for each factor, the inlet pressures *P* were 0.2 MPa, 0.3 MPa and 0.4 MPa; electrostatic voltages *U* were 0 kV, 6 kV and 12 kV; and root core electrode materials *M* were PVC, aluminum and copper, the electrode length was 25 cm; and spray distance *L* was 1.75 m. The specific test factor level is listed in Table 5.

Table 5 Orthogonal factor level table

Level	Inlet pressure *P*/MPa	Electrostatic voltage *U*/kV	Root core electrode material	Spray distance *L*/m
1	0.2	0	PVC	1.75
2	0.3	6	Al	2
3	0.4	12	Cu	2.25

Table 5 was analyzed using the extreme difference method and the results are listed in Table 6. According to Table 6 and the nature of the equal level orthogonal test table, an orthogonal test table was chosen $L_9(3^4)$, and the data measured in the test are listed in Table 7.

Table 6 Orthogonal test results

Test number	*A*	*B*	*C*	*D*	Indicators
	Inlet pressure *P*/MPa	Electrostatic voltage *U*/kV	Root core electrode material	Spray distance *L*/m	Root adhesion increment Δm/g
1	1 (0.2)	1 (0)	1 (PVC)	1 (1.75)	0.283
2	1	2 (6)	2 (Al)	2 (2.00)	0.118
3	1	3 (12)	3 (Cu)	3 (2.25)	0.172
4	2 (0.3)	1	2	3	0.368
5	2	2	3	1	1.640
6	2	3	1	2	0.990
7	3 (0.4)	1	3	2	1.219
8	3	2	1	3	0.791
9	3	3	2	1	2.394

Table 7 Range analysis of orthogonal test results

Test number	*A*	*B*	*C*	*D*	Indicators
	Inlet pressure *P*/MPa	Electrostatic voltage *U*/kV	Root core electrode material	Spray distance *L*/m	Droplet adhesion/g
1	1 (0.2)	1 (0)	1 (PVC)	1 (1.75)	0.283
2	1	2 (6)	2 (Al)	2 (2.00)	0.118
3	1	3 (12)	3 (Cu)	3 (2.25)	0.172
4	2 (0.3)	1	2	3	0.368
5	2	2	3	1	1.640
6	2	3	1	2	0.990
7	3 (0.4)	1	3	2	1.219
8	3	2	1	3	0.791
9	3	3	2	1	2.394
K_{1n}	0.573	1.870	2.064	4.317	
K_{2n}	2.998	2.549	2.880	2.327	7.975
K_{3n}	4.404	3.556	3.031	1.331	
$K_{1n/S}$	0.191	0.623	0.688	1.439	
$K_{2n/S}$	0.999	0.850	0.960	0.776	
$K_{3n/S}$	1.468	1.185	1.010	0.444	
Extreme deviation *R*	1.277	0.562	0.322	0.995	

4 Discussions

4.1 Comparison of the effects of different factors on root fog droplet adhesion

4.1.1 Effect of inlet pressure and electrostatic voltage on root droplet adhesion

The presented work focuses on the adhesion between atomization droplets and roots under different conditions. The success of adhesion between atomization droplets and roots depends on the influence of inlet pressure, electrostatic voltage and electrode materials. Therefore, it is necessary to explore the law between different factors and adhesion amount in the root adhesion test.

The data in Table 3 are plotted in Figure 8, when the inlet pressure was 0.2 MPa, with the increase in electrostatic voltage, the overall weight gain of root droplet adhesion is not obvious. It may be because the target is far from the nozzle, the nozzle outlet flow rate was low, the droplets were more difficult to reach the target, while the electrostatic voltage was low, and the electric field force at a distance was not obvious. However, when the inlet pressure rises to increase, the effect of electrostatic voltage on root droplet adhesion was more and more obvious, indicating that the inlet pressure has an obvious influence on root droplets, especially when the target is far away. Furthermore, when the inlet pressure increases, and thus the droplet particle size is reduced. While, the increase in gas flow rate will help droplet transport to the target near the electrostatic effect on the droplet enhanced.

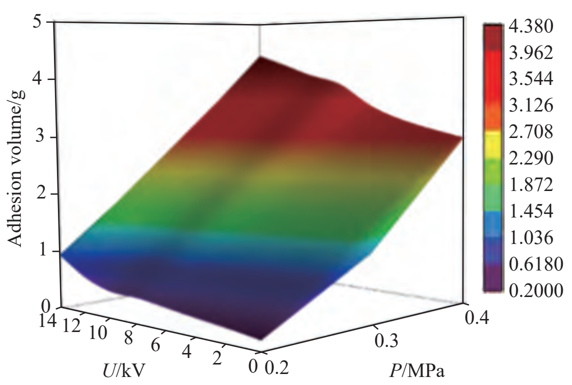

Figure 8 Inlet pressure and electrostatic voltage and root adhesion pattern

As can be seen from Figure 7, when the electrostatic voltage and inlet pressure increased, the particle size of droplets decreased continuously, and the adhesion amounts of roots in Figure 8 showing an increasing trend. Therefore, simulation was used to study the influence of different particle sizes (0.2 mm, 1.0 mm, and 4.0 mm) on the state changes of atomized droplets after hitting the wall and explore the reasons. During the simulation, the contact angle (90°), surface tension (0.072 N/m) and incident velocity (1 m/s) of atomization droplets were set. The simulation results are shown in Figure 9.

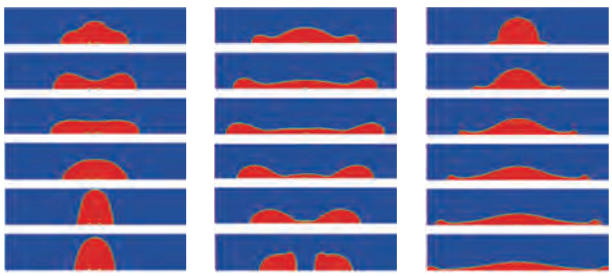

Figure 9 Simulation diagram of atomization droplets' morphological changes after hitting the wall

Figure 8 shows that the larger droplets tend to spread when they hit the wall, and when the spread is large enough, the surface tension is not enough to maintain the droplet shape and fragmentation occurs. The smaller droplets also spread when they hit the wall, but the inertial force is not enough to resist the surface tension, so they do not break. This shows that the larger the particle size, the easier it is to break, and the smaller the droplet adhesion.

4.1.2 Effect of electrostatic voltage and electrode material on root droplet adhesion

From the above analysis, it can be concluded that the influence of the inlet pressure *P* has a more obvious impact on the root adhesion, because the target was far away from the nozzle, the gas pressure was too small, which makes it difficult to distinguish a small amount of adhesion. Here, the inlet pressure was fixed at 0.3 MPa, to measure the effect of different electrostatic voltage *U* and root core electrode material on the root adhesion performance.

Plotting Table 4 into Figure 10 shows that compared with non-metal electrodes, the adhesion of droplets at the roots of metal electrodes has changed more significantly. After turning on the electrostatic module, the root droplet adhesion weight increased by about 0.8 g on average, but the weight difference between the metal electrodes was not significant, indicating that the root core electrode had a certain effect on root droplet adhesion and was related to the material, with the metal electrode having a relatively better effect. The trend of color shift indicates that target deposition with metal electrodes was more sensitive to changes in electrostatic voltage.

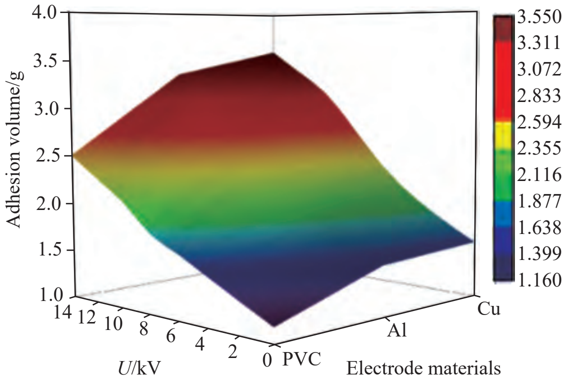

Figure 10 Electrode material and voltage versus root adhesion pattern

To find out whether the droplet deformation in the coupling field is only affected by the flow field, the droplet diameter is 3 mm, the flow rate is controlled at 0.05 m/s, and the droplet deformation in simulation was observed by adjusting the voltage. The droplet deformation was observed by adjusting the voltage, and the measurement results are shown in Figure 11.

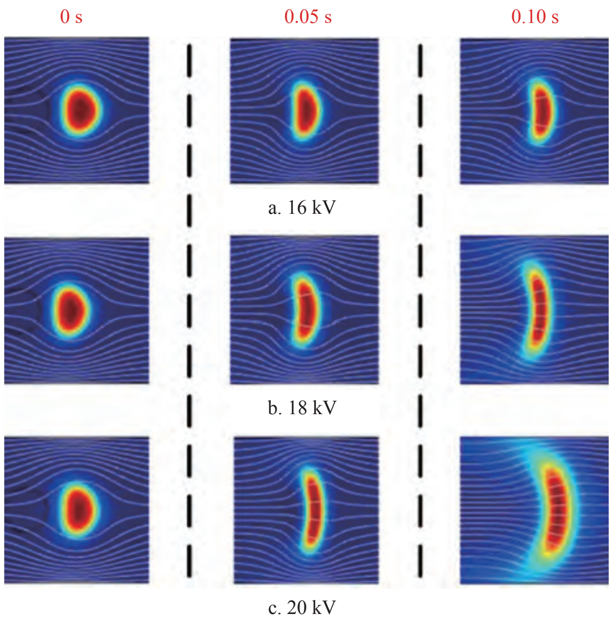

Figure 11 Droplet deformation diagrams after voltage adjustment

It can be seen from Figure 11, that when the inlet velocity was 0.05 m/s, as the electrostatic voltage increases, the effect of voltage on droplet deformation becomes more and more obvious. Therefore, theoretically the higher the electrostatic voltage, the easier the droplet was to deform and break.

4.2 Analysis of extremes of variance method results

In this experiment, the factors that affect the root droplet adhesion in the following order from primary to secondary are: inlet pressure *P*, spray distance *L*, electrostatic voltage *U*, and root core electrode material.

According to the variation pattern of the mean values of the factors, the inlet pressure *P* and the spray distance *L* have an obvious influence on the root droplet adhesion, increasing the inlet pressure and decreasing the spray distance can significantly increase the root droplet adhesion; the electrostatic voltage *U* and the root core electrode material also have a certain influence on the root droplet adhesion. Properly increasing the electrostatic voltage and using metal electrodes can improve the root droplet adhesion to a certain extent, but the improvement was relatively small.

When the inlet pressure P was 0.4 MPa, the spray distance *L* was 1.75 m, the electrostatic voltage *U* was 12 kV and the root core electrode material was copper, the root droplet adhesion was the highest and the effect was the best. The optimal solution was A3B3C3D1.

5 Conclusions

The aim of this research based study was to investigate the effect of the designed high-voltage electrostatic ultrasonic atomization nozzle on the variation pattern of droplet adhesion and root adhesion effect under different operating parameters, as well as the best combination of various influencing factors, and draw the following conclusions:

1) Combining the geometrical and mechanical conditions of the ultrasonic nozzle design, a simple, reliable, low-cost and insulated the high-voltage electrostatic ultrasonic atomization nozzle is designed. Through analyzes of the high-voltage charging methods, the contact charging with the best charging effect is selected. A spiral root core electrode is proposed and a root droplet adhesion test rig is designed aiming at the problems in the process of aeroponics.

2) The comparison results of inlet pressure, electrostatic voltage and electrode material to the root droplet adhesion show that the influence of inlet pressure P had more obvious influence on root droplet adhesion. The larger the particle size, the easier it is to break, and the smaller the droplet adhesion. Compared with non-metallic electrodes, the root droplet adhesion of metal electrodes has a more obvious change, and the target deposition with metal electrodes was more sensitive to the change of electrostatic voltage.

3) The weighing method was used to infer the adhesion of root droplets, the orthogonal test indicates that: the influence of each factor on the adhesion of root droplets in descending order was the inlet pressure *P*, spray distance *L*, electrostatic voltage *U* and root core electrode material. When the inlet pressure P was 0.4 MPa, spray distance *L* was 1.75 m, the electrostatic voltage *U* was 12 kV and the root core electrode material was copper, the root droplets adhesion was the highest and the effect was the best.

Acknowledgements

The authors acknowledge that this work was financially supported by the National Natural Science Foundation of China Program (Grant No. 51975255), Jiangsu Agriculture Science and Technology Innovation Fund (Grant No. CX (18) 3048), and the “Project Funded by the Priority Academic Program Development of Jiangsu Higher Education Institutions (Grant No. 37, (2014))

[References]

[1] Hayden A L, Yokelsen T N, Giacomelli G A, Hoffmann J J. Aeroponics: An alternative production system for high-value root crops. Acta Horticulturae, 2004; 629: 207–213.

[2] Kamies R, Rafudeen M S, Farrant J. The use of aeroponics to investigate

antioxidant activity in the roots of Xerophyta viscosa. Plant Growth Regulation, 2010; 62(3): 203–211.

[3] Rajan R, Pandit A B. Correlations to predict droplet size in ultrasonic atomisation. Ultrasonics, 2001; 39(4): 235–255.

[4] Laryea G N, No S Y. Effect of fan speed and electrostatic charge on deposition of orchard canopy sprays. Atomization & Sprays, 2005; 15(15): 133–144.

[5] Ru Y, Zhou H, Zheng J. Design and experiments on droplet charging device for high-range electrostatic sprayer. Pesticides in the Modern World - Pesticides Use and Management, InTech, 2011. doi: 10.13031/2013. 24589.

[6] Appah S, Wang P, Ou M, Gong C, Jia W. Review of electrostatic system parameters, charged droplets characteristics and substrate impact behavior from pesticides spraying. Int J Agric & Biol Eng, 2019; 12(2): 1–9.

[7] Al-Mamury M, Balachandran W, Al-Raweshidy H, Manivannan N. Computation model of electrostatic spraying in agriculture Industry. Proceedings of the 2014 COMSOL Conference in Cambridge, 2014.

[8] Bren Tj Es A, Pozarlik A K, Brem G. Estimating droplet charge in numerical simulations of charged sprays. Journal of Electrostatics, 2021; 112.

[9] Herrada M A, López-Herrera J M, Gañán-Calvo A M, Vega E J, Montanero J M, Popinet S. Numerical simulation of electrospray in the cone-jet mode. Physical Review E Statistical Nonlinear & Soft Matter Physics, 2012; 86(2): 026305.

[10] Wei W, Zhaolin, Gu, Sheng, Wang, et al. Numerical simulation of the cone–jet formation and current generation in electrostatic spray—modeling as regards space charged droplet effect. Journal of Micromechanics and Microengineering, 2012; 23(1): 15004–15014.

[11] Laryea G N, No S Y. Development of electrostatic pressure-swirl nozzle for agricultural applications. Journal of Electrostatics, 2003; 57(2): 129–142.

[12] Pascuzzi S, Cerruto E. Spray deposition in "tendone" vineyards when using a pneumatic electrostatic sprayer. Crop Protection, 2015; 68: 1–11.

[13] Patel M K, Praveen B, Sahoo H K, Patel B, Kumar A, Singh M, et al. An advance air-induced air-assisted electrostatic nozzle with enhanced performance. Computers and Electronics in Agriculture, 2017; 127: 280–288.

[14] Patel B, Singh M, Mishra P, Manes G, Patel M. Efficacy of the prototype electrostatic nozzle for cotton crops. African Entomology, 2021; 29(2): 471–478.

[15] Gao J, Zhang J, Lu D. Design and atomization experiments of an ultrasonic atomizer with a levitation mechanism. Applied Engineering in Agriculture 2016; 32(4): 353–360.

[16] Chen J, Jiang W, Han C, Liu Y. Study on supersonic swirling condensation characteristics of CO_2 in Laval nozzle. Journal of Natural Gas Science and Engineering, 2020; 84: 103672.

[17] Gao X, Li C, Zhang D, Gao H, Han X. Numerical analysis of the activated combustion high-velocity air-fuel (AC-HVAF) thermal spray process: A survey on the parameters of operation and nozzle geometry. Surface and Coatings Technology, 2021; 405: 126588. doi: 10.1016/j.surfcoat.2020.126588.

[18] Suleymanov M A, Tsoy O A. Research of gas jet pumps with diagraphic, conical and laval nozzles. Oil and Gas Technologies, 2020; 129: 53–57.

[19] Hansmann B R, Abel B. Kinetics in cold laval nozzle expansions: From atmospheric chemistry to oxidation of biomolecules in the gas phase. ChemPhysChem, 2010; 8(3): 343–356.

[20] Planche MP, Khatim O, Dembinski L, Bailly Y, Coddet C. Evaluation of the splats properties and relation with droplets diameters in atomization process using a De Laval Nozzle. Materials Chemistry and Physics, 2013; 137(3): 681–688.

[21] Kudryavtsev Y, Ferrer R, Huyse M, Bergh P, Duppen P V. The in-gas-jet laser ion source: resonance ionization spectroscopy of radioactive atoms in supersonic gas jets. Nuclear Instruments & Methods in Physics Research, 2013; 297: 7−12.

[22] Zadvornaya A, Creemers P, Dockx K, Ferrer R, Papadakis P. Characterization of supersonic gas jets for high-resolution laser ionization spectroscopy of heavy elements. Physical Review X, 2018; 8(4): 041008. doi: 10.1103/PhysRevX.8.041008.

[23] Sallam K A, Aalburg C, Faeth G M. Breakup of round nonturbulent liquid jets in gaseous crossflow. AIAA Journal, 2004; 42(12): 2529–2540.